






Localization of a Medial Temporal Lobe—Precuneus Network for Time Orientation

Jax Skye, PhD  ,^{1,2,3,4} Joel Bruss, BA,^{1,2} Guillaume Herbet, PhD ,^{5,6}
Daniel Tranel, PhD,^{1,4} and Aaron D. Boes, MD, PhD  ^{1,2,3}

Objective: Time orientation is a fundamental cognitive process in which one's personal sense of time is matched with a universal reference. Time orientation is commonly assessed through mental status examination, yet its neural correlates remain unclear. Large lesions have been associated with deficits in time orientation, but the regional anatomy implicated in time disorientation is not well established. The current study investigates the anatomy of time disorientation and its network correlates in patients with focal brain lesions.

Methods: Time orientation was assessed 3 months or more after lesion onset using the Benton Temporal Orientation Test (BTOT) in 550 patients with acquired, focal brain lesions, 39 of whom were impaired. Multivariate lesion-symptom mapping and lesion network mapping were used to evaluate the anatomy and networks associated with time disorientation. Performance on a variety of neuropsychological tests was compared between the time oriented and time disoriented group.

Results: Lesion-symptom mapping showed that lesions of the precuneus, medial temporal lobes (MTL), and occipito-temporal cortex were associated with time disorientation ($r = 0.264$, $p < 0.001$). Lesion network mapping using normative connectome data demonstrated that these regional findings occurred along a network that includes white and gray matter connecting the precuneus and MTL. There was a strong behavioral and anatomical association of time disorientation with memory impairment, such that the 2 processes could not be fully disentangled.

Interpretation: We interpret these findings as novel evidence for a network involving the precuneus and the medial temporal lobe in supporting time orientation.

ANN NEUROL 2023;94:421–433

Humans perceive time as flowing continuously from past through present to future. Time orientation describes the ability to match one's internal representation of time to a universal reference system, or "clock time", on the order of hours to years.^{1,2} Time disorientation can occur in a wide variety of neurological and psychiatric disorders.³ Identifying this impairment is useful in understanding a patient's overall cognitive status as it is often associated with other aspects of cognition including

planning,⁴ decision making,⁵ and memory.^{6,7} Time orientation is frequently assessed, yet little is known about the underlying neural substrates. This study investigates time disorientation following focal, acquired brain lesions.

Elucidating the anatomy most critical to representing the passage of time and associating it with clock time has proven challenging. Unlike many basic perceptual systems, there is no clear sensory receptor for time: the source of information the brain uses to estimate time

View this article online at [wileyonlinelibrary.com](https://onlinelibrary.wiley.com). DOI: 10.1002/ana.26681

Received Aug 12, 2022, and in revised form Apr 26, 2023. Accepted for publication May 2, 2023.

Address correspondence to Skye, PhD, Department of Neurology, University of Iowa Carver College of Medicine, University of Iowa, 200 Hawkins Dr. GH W229 Iowa City, IA 52242, USA. E-mail: jax-skye@uiowa.edu

From the ¹Department of Neurology, University of Iowa Carver College of Medicine, University of Iowa, Iowa City, Iowa, USA; ²Department of Pediatrics, University of Iowa Carver College of Medicine, University of Iowa, Iowa City, Iowa, USA; ³Department of Psychiatry, University of Iowa Carver College of Medicine, University of Iowa, Iowa City, Iowa, USA; ⁴Department of Psychological and Brain Sciences, University of Iowa, Iowa City, Iowa, USA; ⁵Institute of Functional Genomics, University of Montpellier, CNRS, INSERM, Montpellier, France; and ⁶Department of Neurosurgery, Montpellier University Medical Center, Gui de Chauliac Hospital, Montpellier, France

is unclear but presumed to be multimodal. Previous research has indicated there is a robust association of time disorientation and amnesia, which highlights a potential role for medial temporal lobe (MTL) structures.^{7–10} Yet other studies suggest time disorientation may also have features that are separable from amnesia.^{11–13} Other regional anatomy that has been implicated in time orientation includes the mediodorsal nucleus of the thalamus,^{14,15} the right cerebral hemisphere,¹⁶ the precuneus,¹⁷ and the prefrontal cortex.¹⁷ The extent to which these regional associations are correlational or causal is unclear, as is the relative contribution of each region.

Studying patients with focal, acquired brain lesions who are impaired in time orientation has the potential to aid in the elucidation of brain regions most critical for supporting time orientation. To date most lesion studies of time disorientation have been limited by small sample sizes.^{14,15,18,19} Time disorientation after brain injury is relatively common in the acute epoch, but spontaneously resolves in ~95% of patients within about 6 weeks, leaving only a small percentage with a chronic impairment.²⁰ To date, a large-scale lesion-symptom mapping study of chronic time disorientation has not been performed. In addition to investigating lesion location, lesions and associated symptoms can also be interpreted in the context of disrupting a broader network that extends beyond the anatomical boundaries of the lesion.²¹ Lesion network mapping is an approach that combines traditional lesion-symptom mapping approaches with structural and/or functional connectivity information derived from large normative “connectome” datasets to evaluate lesion associated networks.^{21,22} These approaches have not yet been applied to time orientation.

Here, we utilize a large registry of 550 patients with focal, acquired brain lesions, who have standardized time orientation assessments performed more than 3 months after the lesion onset. Our goals were to perform a data-driven analysis evaluating the regional anatomy and networks associated with time disorientation along with evaluating the cognitive profile of individuals with time disorientation relative to a brain-damaged comparison group.

Methods

We used neuropsychological test data and neuroimaging data available through the Iowa Neurological Patient Registry to perform our analyses. Patients in the Registry gave informed, written consent prior to participation in this study, and the study was approved by the Institutional Review Board of the University of Iowa. Data were collected >3 months after lesion onset in adult patients 18 or

older. Patients with focal, acquired brain lesions with visible borders were included regardless of etiology. Patients were screened and excluded if pre-existing psychiatric and neurological conditions were present. Following enrollment, patients underwent comprehensive neuropsychological evaluation in accordance with Benton Neuropsychology Laboratory protocols,²³ which included an extensive battery of neuropsychological tests designed to assess major domains of cognition and behavior. For the current analysis, in order to ensure that measured time disorientation was not confounded by receptive language deficits, patients were excluded from this study if they had impaired scores on the Boston Diagnostic Aphasia Examination (BDAE) Complex Ideational Material Test, the Multilingual Aphasia Examination (MAE) Token Test, or the MAE Aural Comprehension Test (defined as raw scores ≤ 8 , ≤ 36 , or ≤ 14 , respectively).

We used the Benton Temporal Orientation Test (BTOT) to measure time orientation.^{24,25} In this test, the examiner verbally asks the patient 5 questions about where they are in time (Table 1). A total of 625 patients were given a score on a scale from 0 to –113 with 0 being considered unimpaired performance. The BTOT score obtained most contemporaneously with the date of the patient’s research brain scan was used if a patient had been administered the BTOT more than once. Patients with a score of 0 constitute the brain-damaged comparison group ($n = 511$). Following the normative standards for the BTOT,²⁴ patients in our study with a score of –3 or worse were considered impaired; there were 39 such patients (mean score = –15.10, standard deviation = –22.33, range = –3

Table 1. The Benton Temporal Orientation Test (BTOT) Asks 5 Questions about Where a Person Is in Time

Benton Temporal Orientation Test		
Time Interval	Scoring Criteria	Maximum Error
Month	–5 Points per month off	–30 Points
Day of the month	–1 Points per day off	–15 Points
Year	–10 Points per year off	–60 Points
Day of the week	–1 Points per day off	–3 Points
Time of day	–1 Points per half hour off	–5 Points

Note: If an incorrect response is provided, a specified number of points is deducted from a starting score of 0 according to the nature of their error. Each time interval has a maximum deduction for that item.

to -102). Since the degree of temporal disorientation does not scale with BTOT score (e.g., a patient being off by 1 year receiving a score of -10 is not thought to be “twice as disoriented” as a patient being off by 1 month and receiving a score of -5), binarized scores for time oriented and time disoriented patients were used as the behavioral variable for all analyses. We excluded 75 patients with a score of -1 or -2 from the main analyses, which created a greater contrast between the impaired and unimpaired groups; these scores correspond to common errors healthy adults make in self-referential timing (e.g., being 30 min off for the current time or being a day off for the day of the week) and are not “impaired” according to the normative standards for the BTOT. Five hundred fifty participants met the criteria for this study (Table 2). We used a *t*-test to compare the age, education, and lesion volume between time oriented and time disoriented patients.

Structural neuroimaging was obtained 3 months or more after the lesion onset and the boundaries of the lesions were manually segmented for all 550 scans using standard procedures.²⁶ Lesion masks for neuroimaging data acquired prior to 2006 were generated using the MAP-3 method^{26,27} wherein the boundaries of the lesion are traced onto a template brain. Data acquired in 2006 and after were manually traced onto the patient’s T1 native scan in FSL²⁸ and then subsequently transformed into MNI152 space using Advanced Normalization Tools (ANTs). The anatomical accuracy of the native trace and the transformed lesion mask were confirmed and edited as needed by a neurologist (A.D.B.) who was blind to all demographic and cognitive data.

Lesion-symptom mapping was used to identify regions of damage associated with time disorientation. LESYMAP, a multivariate lesion-symptom mapping technique that uses sparse canonical correlation analysis for neuroimaging (SCCAN), was employed using binary BTOT data.²⁹ The LESYMAP algorithm identifies multivariate correlations of lesion anatomy and behavioral data and then performs a within-cohort fourfold cross validation analysis to assess the statistical significance of the statistical map based on its ability to make accurate predictions in the left out sample. This within-cohort validation step performs optimally if impaired and unimpaired groups are relatively matched in sample size. For this analysis, each time disoriented patient was matched with 3 time-oriented patients that were selected from the cohort with unimpaired BTOT performance based on having the closest lesion volume ($n = 156$). This comparison group simultaneously improved the ratio of impaired to unimpaired subjects for the within-cohort validation

and controlled for lesion volume. Functional lesion network mapping was performed using 2 complimentary approaches, one that derives networks from regional peaks of a lesion-symptom map^{22,30} and the other that uses each individual lesion volume as a seed region to generate a network, with subsequent application of a linear model to identify network correlates of behavior.^{31,32} For both approaches the same resting state functional connectivity MRI (rs-fcMRI) data from a normative database were used, as in previous work ($n = 98$ healthy right-handed subjects; 48 male subjects, age 22 ± 3.2 years).³³ The rs-fcMRI data were processed in accordance with previously described methods.³⁴ Briefly, participants completed 2 6.2-min rs-fcMRI scans during which they were asked to rest in the scanner (3T, Siemens) with their eyes open (repetition time [TR] = 3,000 ms, echo time [TE] = 30 ms, flip angle [FA] = 85° , 3 mm voxel size [27 mm³], field of view [FOV] = 216, 47 axial slices with interleaved acquisition and no gap). Functional data were acquired at 3 mm voxel size and spatially smoothed using a Gaussian kernel of 4 mm full-width at half-maximum. The data were temporally filtered ($0.009 \text{ Hz} < f < 0.08 \text{ Hz}$) and several nuisance variables were removed by regression. Inclusion of the first temporal derivatives of the regressors within the linear model accounted for the time-shifted versions of spurious variance. The time course of the average blood-oxygen-level-dependent (BOLD) signal within each seed ROI was compared with the BOLD signal time course of other brain voxels to identify regions with positive and negative correlations. Pearson correlation coefficients were converted to normally distributed *z*-scores using the Fisher transformation. To incorporate the 98 individual *z*-score maps a group mean *t*-test was performed separately for the positive and negative maps of *z*-scores using FSL FLAMEO using ordinary least-squares.

In the first approach, networks are derived from brain areas representing the strongest brain-behavior associations identified from the lesion-symptom map. This allows visualization of the network associated with the brain region(s) most implicated in the behavioral impairment while avoiding some of the problems associated with BOLD signal averaging from large lesion “seeds”.³⁵ For this approach 4 6 mm diameter spherical regions of interest (ROIs) were placed at grey matter regional peaks from the LESYMAP analysis. The other 2 ROIs from the lesion-symptom map were predominantly in white matter and they were not included in the functional lesion network mapping. To identify the functional network that best represents these individual rs-fcMRI maps, we

Table 2. Demographic Information for Patients in This Study

Characteristic	Demographics		
	All Patients (N = 550)	Time Disoriented (n = 39)	Time Oriented (n = 511)
Age in years			
Mean (std)	52.4 (14.5)	59.7 (14.9)	51.9 (14.3)
Education in years			
Mean (std)	13.4 (2.75)	13.2 (3.15)	13.4 (2.72)
Gender			
Female	268	19	249
Male	282	20	262
Handedness			
Right	493	34	459
Left	41	4	37
Mixed	16	1	15
Race			
African American	4	0	4
American Indian	3	0	3
Caucasian	541	39	502
Other/unknown	2	0	2
Ethnicity			
Hispanic	2	0	2
Non-Hispanic	547	39	508
Unknown	1	0	1
Lesion volume in mm ³			
Mean (std)	37,800 (5650)	64,500 (76,700)	35,700 (54,200)
Lesion laterality			
Right	205	13	192
Left	228	7	221
Bilateral	117	19	98
Etiology			
Ischemic stroke	287	17	270
Hemorrhage	119	7	112
Benign tumor resection	78	4	74
Other resection	29	3	26
Focal contusion	17	3	14
Herpes simplex or limbic encephalitis	12	5	7
Multiple etiologies	8	0	8

employed a weighted principal component analysis in MATLAB, as performed previously.²²

For the second approach, each lesion mask was entered as a “seed” ROI to generate a brain-wide network map of *z*-scores representing the voxel-wise positive and negative correlations with the average BOLD signal time course within the lesion volume. All 550 resulting network maps and corresponding behavioral results were included in a permutation-based voxel-wise 2-tail linear model using 2000 permutations with tail approximation and Threshold Free Cluster Enhancement employed via FSL PALM as previously described^{31,32,36} (<https://fsl.fmrib.ox.ac.uk/fsl/fslwiki/Randomise/UserGuide>).

Structural lesion network mapping was performed using DSI Studio. Each lesion mask was used as a “seed” ROI for a deterministic tractography analysis using normative diffusion MRI data. This produces a streamline map of white matter tracts likely to be affected, or disconnected, by a lesion, as performed previously.²² The analysis was performed using high quality DTI data included in the Human Connectome Project’s MGH 32-fold group connectome (<https://ida.loni.usc.edu/login.jsp>).³⁷ As described above for the fcMRI analysis, all 550 voxel-wise streamline maps and corresponding behavioral data were included in a permutation-based voxel-wise 2-tail linear model via FSL PALM. Results from the latter 2 analyses were corrected for multiple comparisons using false discovery rate.

To evaluate whether cognitive impairments co-occur with time disorientation, the distribution of scores for neuropsychological tests was compared to the distribution of scores in the brain-damaged comparison group. This analysis focused on individual tests available for at least 75% of the time disoriented patients. Linear regression was used to compare tests with continuous scores using age and lesion volume as covariates and Pearson’s chi squared test was used for categorical scores. Several of the cognitive tests used in our analyses were subtests from the Wechsler Adult Intelligence Scale (WAIS), the most widely used measure of adult intelligence.³⁸ If a participant was administered multiple versions of the WAIS, the most recent version was used.³⁹

Post-Hoc Analyses

We performed a post-hoc analysis of lesion location for time disoriented participants with relatively intact cognitive performance, which we defined as being in the normal range (not more than 1 standard deviation below the mean) on >75% of the neuropsychological tests included in this study. Lesion location was evaluated in this subgroup analysis using proportional subtraction as the sample size was underpowered for a LESYMAP analysis.

Participants were divided into impaired (BTOT score of -3 or worse) and unimpaired (BTOT score of 0) groups. The proportional metric (PM) was calculated with FSL⁴⁰ by creating a difference map between the proportion of time disoriented patients and proportion of time oriented patients at each voxel, such that voxels were weighted from -1 to 1.⁴¹ Higher scores indicated a stronger relationship between damage at that voxel and time disorientation. We performed a related post-hoc analysis with a focus on memory performance rather than overall cognitive performance. For this, Rey Auditory Verbal Learning Test (AVLT) and Rey-Osterrieth Complex Figure Test (CFT) recall scores were used to identify time disoriented patients who had relatively intact memory, defined as a score within 2 standard deviations of the age-corrected normative mean on both tests for inclusion in a proportional subtraction map.

In addition, we performed a retrospective chart review of 16 patient records from surgical patients after resection of benign tumors that resulted in damage to the precuneus to evaluate for potential subjective changes in the perception of time.

Results

A total of 39 individuals with time disorientation were identified. Relative to the lesion volume matched brain-damaged comparison group, on average those with time disorientation were older ($\bar{x}_{\text{time oriented}} = 48.0 \pm 15.4$, $\bar{x}_{\text{time disoriented}} = 59.7 \pm 14.9$; $p < 0.001$), adequately matched for lesion size ($\bar{x}_{\text{time oriented}} = 61,485 \pm 66,854$, $\bar{x}_{\text{time disoriented}} = 64,524 \pm 76,717$; $p = 0.836$), had a higher rate of bilateral lesions (48.7 vs. 22.2%, $X^2(1, N = 156) = 8.76$, $p = 0.00309$), and had a higher rate of encephalitis (30.8–2.56%, $X^2(1, N = 156) = 23.6$, $p < 0.001$). In the impaired group, 15 individuals had lesions involving posteromedial cortices and 9 patients had a stroke of the posterior cerebral artery distribution (3 left hemisphere, 3 right hemisphere, and 3 bilateral). Seven patients had lesions in the frontal lobe, mostly involving the ventromedial prefrontal cortex, 5 patients had encephalitis, 1 patient had a right putamen lesion, and 2 lesions involved the thalamus that intersected with the mediodorsal nucleus of the thalamus. The distribution of lesion masks of all 550 participants in this study, which spanned virtually the entire cortex, is shown in Fig. 1. Of the 550 participants, a maximum overlap of 51 lesions was observed in the right frontal white matter. Lesions of the 39 individuals with time disorientation are shown in Fig. 1B. The overlap map of the 75 patients with BTOT scores of -1 and -2 that were not included in the main analysis showed a similar distribution to the brain-damaged comparison group (Fig. 1C).

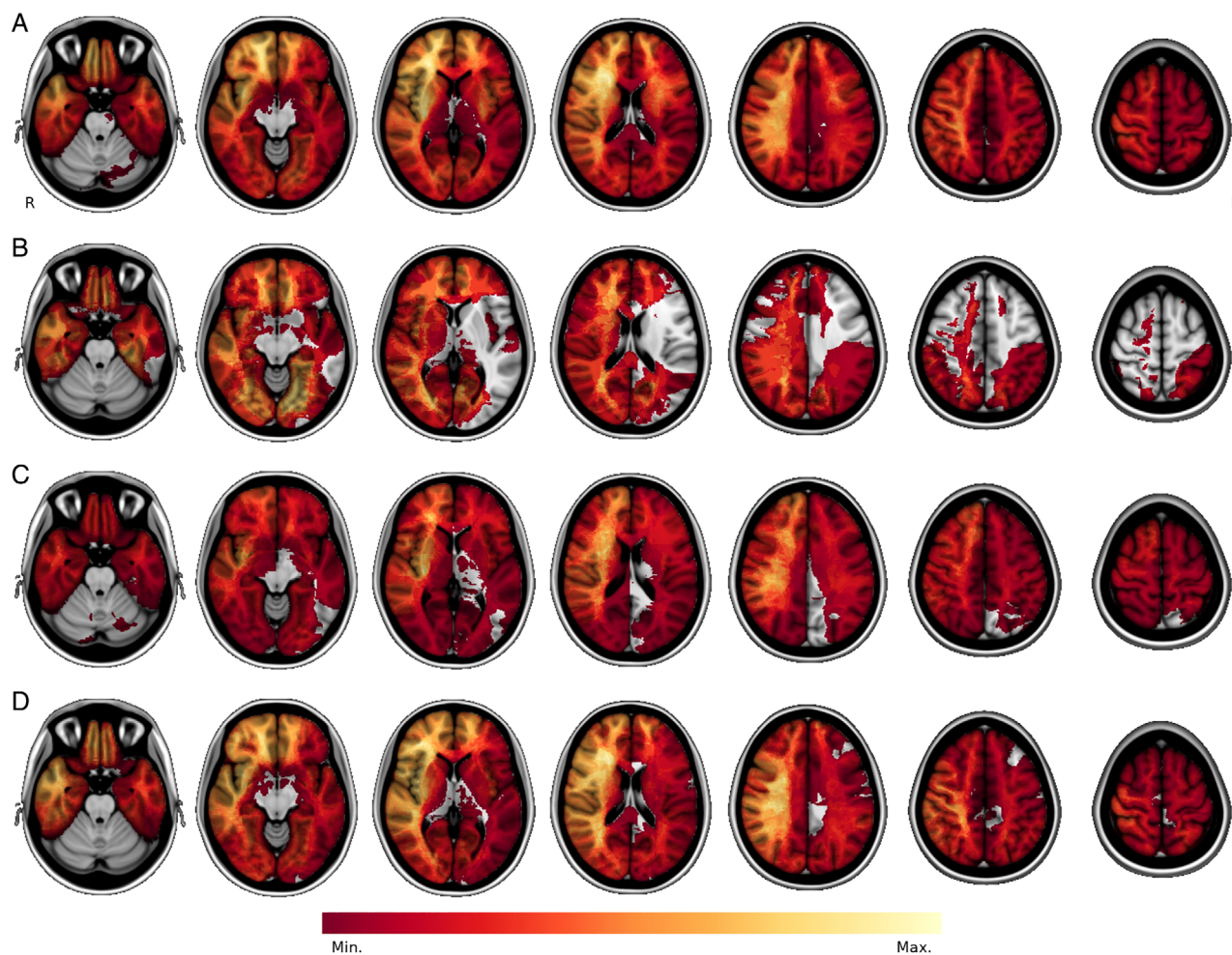


FIGURE 1: (A–D) Lesion masks of all 550 participants in this study were overlapped to show that we have lesion coverage across a majority of the brain to assess brain-behavior relationships (axial slices $-24, -10, 4, 18, 32, 46, 60$; A). The maximum number of overlapping lesions (51) was located in right frontal white matter. The lesion masks of the 39 time disoriented participants are shown in B; the region of peak overlap in the left parahippocampal gyrus contained 9 lesions. Seventy-five individuals had a score of 1 or 2 on the benton temporal orientation test and were excluded from this analysis. The distribution of these patients' lesions is similar to the time oriented group and the voxel of peak lesion overlap (19 lesions) is also in right frontal white matter (C). The lesion volume matched brain-damaged comparison group used for the lesion-symptom mapping analysis ($n = 156$), had a peak lesion overlap of 24 lesions in right frontal white matter, and showed a similar distribution of lesions as the full cohort ($N = 550$; D). [Color figure can be viewed at www.annalsofneurology.org]

The lesion-volume matched brain damage comparison group used for the lesion-symptom map showed a similar distribution (Fig. 1D).

Lesion-Symptom Mapping Results

The lesion-symptom mapping analysis of time was significant at $r = .264, p < 0.001$ (Fig. 2). The strongest peak regional findings occurred at right and left precuneus (MNI coordinates $22-60\ 38; -21\ -61\ 21$; and $-18\ -71\ 40$), left parahippocampal gyrus ($-25-29\ -20$), right hippocampus ($29\ -25\ -12$), right and left visual association cortex ($19-71\ -4$ & $-17\ -66\ -10$, respectively), and deep right frontal white matter ($19\ 36\ 20$).

Lesion Network Mapping Results

A 6 mm diameter spherical ROI was placed over the most significant local maxima within a grey matter mask of the lesion-symptom map. Four regional gray matter peaks were identified in the left parahippocampal gyrus ($-25-29\ -20$), right hippocampus ($29\ -25\ -12$), left precuneus ($-21-61\ 21$), and left visual association cortex ($-17-66\ -10$). The principal component network derived from these regions is shown in Fig. 3A,B, with the most robust findings in the ventral precuneus, MTL, and occipital lobe. This network overlapped with visual and default mode networks.

The functional lesion network mapping produced using FSL PALM appeared similar. This network also included regions of the precuneus, MTL, and occipital

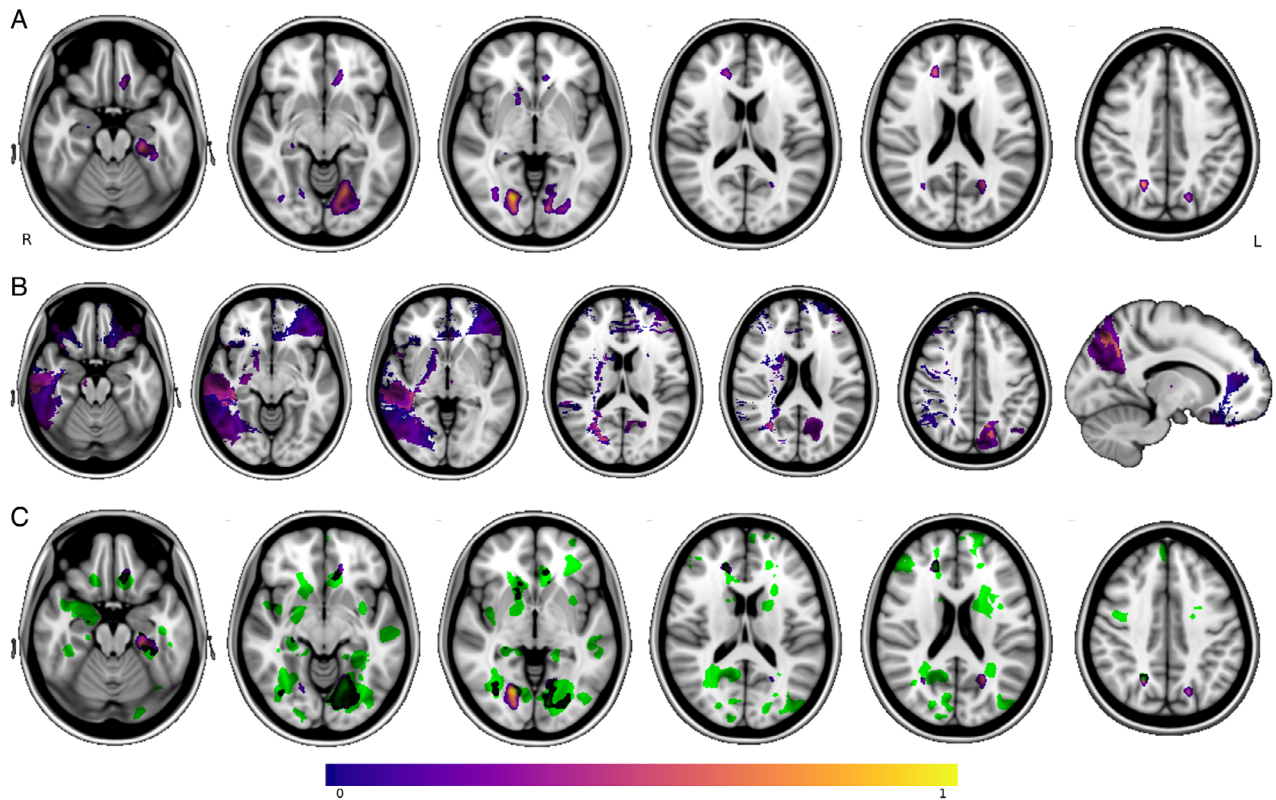


FIGURE 2: (A–C) The lesion-symptom mapping analysis showed the strongest regions of peak intensity in the precuneus, medial temporal lobe, and visual association areas bilaterally in addition to the left straight gyrus (A; axial slices -20 , -9 , -3 , 16 , 20 , 40). (B) The left posterior precuneus is more likely to be damaged in time disoriented patients without severe memory impairment compared to those oriented to time (same axial slices as A, sagittal slice -13). Regions associated with memory impairment as measured by the 30-min recall trials of the AVLT and CFT are shown in C in green. The time disorientation lesion-symptom map was overlaid, showing no overlap between regions associated with memory and time orientation in the left precuneus and little overlap in right visual association areas. [Color figure can be viewed at www.annalsofneurology.org]

lobe (Fig. 3C,D). The structural lesion network map revealed a white matter tract extending between the posterior precuneus and parahippocampal gyrus associated with time disorientation (Fig. 3E,F). All FSL PALM results displayed in Fig. 3C–F were significant at a false discovery rate of 5%.

Evaluation of Co-occurring Cognitive and Memory Impairment

To characterize cognitive impairments that co-occur with time disorientation, we compared the distribution of scores between the impaired ($n = 39$) and brain-damaged comparison ($n = 511$) groups across a variety of neuropsychological tests (Table 3). Age and lesion volume were included as covariates in our linear regression given significant between-group differences. After correcting for multiple comparisons, the Bonferroni corrected α was 0.002. The group with time disorientation performed worse on most tests.

Based on the observation of differences in cognitive performance in the individuals with impaired time orientation, post-hoc analyses were performed. We aimed to

address an alternative explanation that our neuroanatomical findings of the lesion-symptom maps may reflect global cognitive impairment or memory impairment rather than our primary function of interest, time orientation. We identified 11 time disoriented patients with relatively preserved cognition (defined as impaired on fewer than 25% of the neuropsychological tests in Table 3). A proportional subtraction analysis was performed on this cohort with a peak regional finding at the left precuneus (Fig. 4). Next, we did an analysis specifically looking at individuals with time-disorientation without severe impairments in memory (performance within 2 standard deviations of normative performance). While this group was selected for having relatively preserved memory it is notable memory still differed between this cohort and the brain-damaged comparison group ($n = 511$) (AVLT 30-min recall $t(9) = 1.23$, $p = 0.25$; Complex Figure 30-min recall $t(9) = 2.19$, $p = 0.055$). The small sample size likely contributed to the lack of statistical significance in memory between these samples. The proportional subtraction analysis demonstrated that time disoriented patients without severe memory impairment ($n = 10$) had proportionally

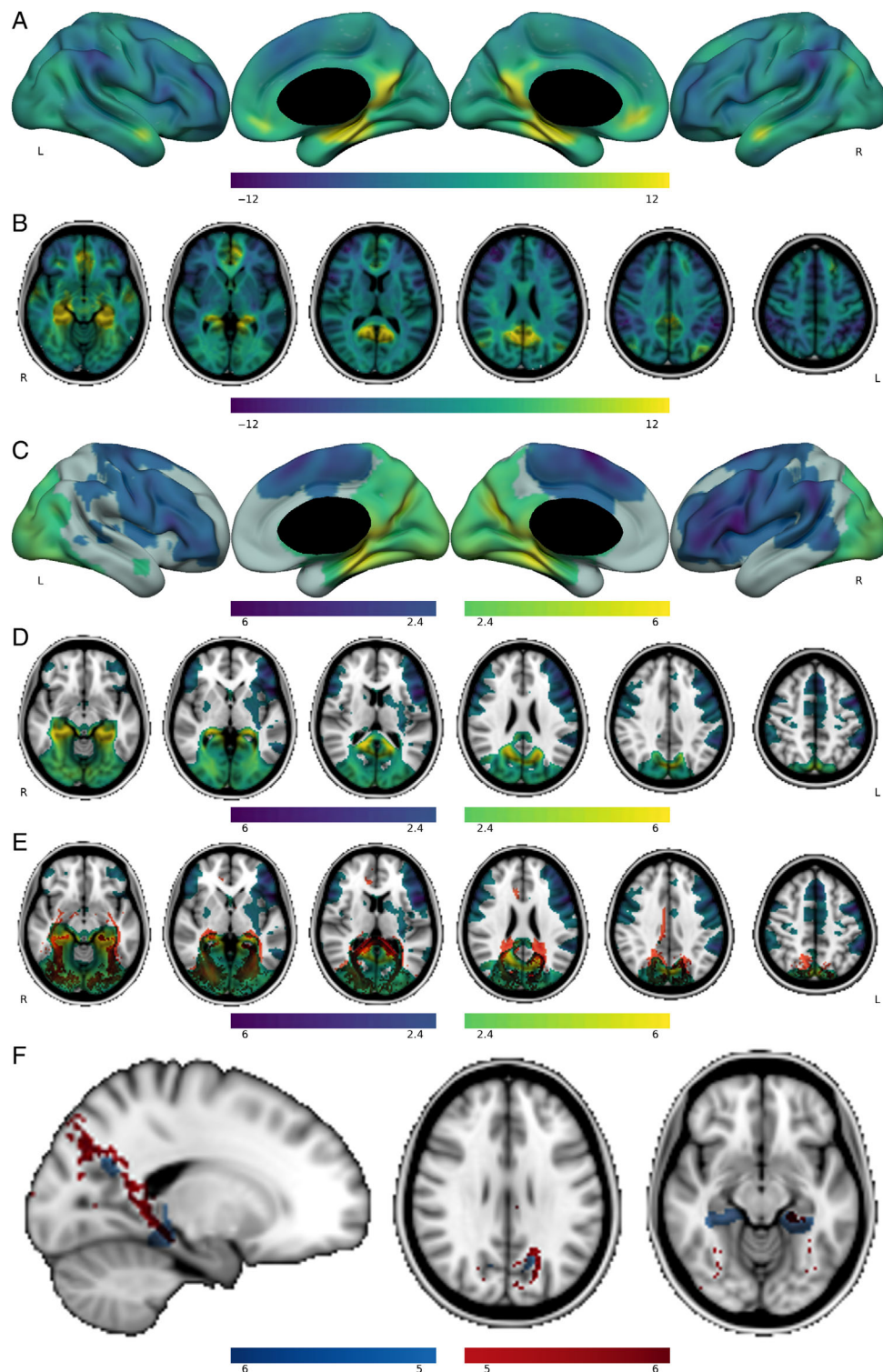


FIGURE 3: (A, B) The principal component network derived using normative rs-fcMRI from peak regional findings in the time orientation lesion-symptom map, showing network involvement of the precuneus, MTL, and occipital lobe (z-scores shown, axial slices -12, 0, 12, 24, 36, 48). (C, D) show functional lesion network mapping results produced using FSL PALM which shows a largely similar pattern of network involvement (t-scores shown) and anti-correlated regions. (E) The structural lesion network mapping result from PALM in red and the functional lesion network map depicted in D, revealing a bilateral white matter tract connecting the medial temporal lobes to the precuneus that largely overlaps with the functional lesion network map. (F) The functional (in blue) and structural (in red) lesion network maps thresholded to t-scores >5, which highlights a white matter tract connecting the precuneus to the MTL (sagittal slice -18, axial slices -12 and 28) that overlaps with peak regions from the functional lesion network map. [Color figure can be viewed at www.annalsofneurology.org]

Table 3. Distribution of Neuropsychological Test Scores between the Time Oriented and Time Disoriented Groups with Linear Regression Using Age and Lesion Volume as Covariates**Comparing Neuropsychological Test Scores Between groups**

Neuropsychological Test	Time Disoriented Group	Brain-Damaged Comparison Group	<i>p</i> -Value
	Mean Score (std)	Mean Score (std)	
Arithmetic (WAIS) ^a	8.59 (2.24)	10.0 (2.98)	< 0.001
Rey Auditory-Verbal Learning Test			
Trial 1 ^a	4.43 (1.48)	5.66 (1.89)	< 0.001
Trial 2 ^a	6.00 (2.00)	7.93 (2.27)	< 0.001
Trial 3 ^a	9.97 (2.19)	9.34 (2.56)	< 0.001
Trial 4 ^a	7.59 (3.04)	10.5 (2.58)	< 0.001
Trial 5 ^a	8.05 (3.18)	11.2 (2.59)	< 0.001
30-min Delayed Recall ^a	3.92 (3.65)	8.87 (3.39)	< 0.001
Recognition ^a	10.1 (4.38)	13.7 (1.84)	< 0.001
Benton Facial Recognition Test ^a	40.8 (6.17)	44.8 (4.60)	< 0.001
Benton Visual Retention Test (number of errors) ^a	9.91 (4.95)	5.31 (4.47)	< 0.001
Block Design (WAIS) ^a	8.82 (2.99)	10.4 (4.74)	< 0.001
Boston Naming Test ^a	46.1 (14.5)	54.3 (5.32)	< 0.001
Clock Drawing Test ^a	2.14 (0.891)	1.42 (0.712)	< 0.001
Rey-Osterrieth Complex Figure			
Copy ^a	25.3 (6.49)	30.4 (4.94)	< 0.001
Recall ^a	8.15 (6.40)	17.1 (6.71)	< 0.001
Time to Complete ^a	5.33 (2.45)	3.35 (1.58)	< 0.001
Digit-Symbol Coding (WAIS) ^a	7.14 (2.75)	9.41 (2.89)	< 0.001
Judgment of Line Orientation ^a	22.8 (5.54)	25.2 (4.36)	< 0.001
Orientation to Personal Information ^a	3.79 (0.469)	3.98 (0.148)	< 0.001
Place Orientation ^a	1.77 (0.524)	2.00 (0.185)	< 0.001
Clinical Assessment of Articulation	1.13 (0.341)	1.16 (0.466)	= 0.345
Clinical Assessment of Fluency	1.13 (0.341)	1.08 (0.345)	= 0.013
Clinical Assessment of Paraphasias	1.19 (0.543)	1.18 (0.508)	= 0.981
Clinical Assessment of Prosody	1.26 (0.575)	1.17 (0.497)	= 0.426
Controlled Oral Word Association Test	31.6 (11.5)	36.5 (12.2)	= 0.031
Digit Span (WAIS)	8.77 (3.01)	9.38 (2.78)	= 0.354
Information (WAIS)	8.77 (2.33)	10.2 (2.92)	= 0.006
Similarities (WAIS)	9.47 (3.14)	10.6 (2.83)	= 0.029

^aSignificant after Bonferroni correction.

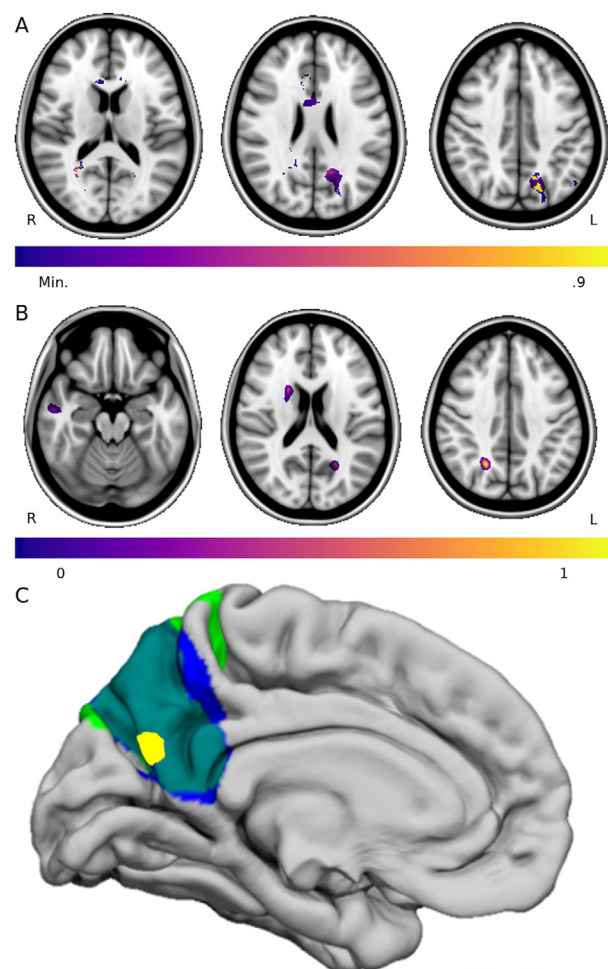


FIGURE 4: (A–C) A proportional subtraction analysis of 11 time disorientated patients with relatively unimpaired cognitive performance in other domains was conducted ($PM = 0.96$ in the precuneus at MNI coordinates $-13, -61, 37$) (A; axial slices 15, 25, 40). (B) (axial slices $-18, 20,$ and 39) The lesion-symptom map of time orientation covarying for memory performance. The strongest regional peaks are in white matter deep to the right precuneus ($22-59\ 39$), the left posterior precuneus ($-21-60\ 20$), white matter deep to the superior part of the head of the caudate nucleus ($21\ 9\ 20$), and the right superior temporal sulcus ($55-9\ -18$). (C) The lesion location of 2 individuals with tumor resection surgeries are shown (in blue and green, with overlap of the 2 lesions in turquoise). Both individuals had lesions that overlapped with our lesion-symptom mapping results in the precuneus and spontaneously reported major alterations in their experience of time following the lesion. The lesion-symptom mapping result is just deep to the cortical surface and a yellow marker is shown to denote the location on this surface view. [Color figure can be viewed at www.annalsofneurology.org]

more damage to the left precuneus compared to time oriented patients ($n = 511$; Fig. 2B).

To further evaluate how lesion location relates to memory impairment versus time disorientation, we also performed multivariate lesion-symptom mapping of the 30-min delayed recall trial of the AVLT ($n = 526$) and 30-min delayed recall trial of the CFT ($n = 521$) and

qualitatively compared the resulting maps to that of time disorientation (Fig. 2C). This revealed several highly overlapping regions of the medial temporal lobe and occipito-temporal regions. Regional peaks associated with memory impairment were in the right precuneus ($22-60\ 39$), left parahippocampal gyrus ($-25-29\ -20$), right hippocampus ($29\ -25\ -12$), right visual association cortex ($19-71\ -4$) and left visual association cortex ($-17-66\ -10$), and deep right frontal white matter ($19\ 36\ 20$). Notably, the left precuneus region was present in the time disorientation lesion-symptom map but not present in the memory maps. In addition, we repeated our main lesion-symptom map of the BTOT while covarying for memory. We used linear regression to covary for a composite z-score reflecting memory performance. This was derived from the 30-min delayed recall trials of the AVLT and CFT. Not all individuals had memory tests, so the sample size was reduced ($n = 156$). The time orientation scores after regressing out memory were entered in a lesion-symptom mapping analysis that produced a similar spatial distribution of findings with regional peaks in the precuneus (Fig. 4:B), but this map did not reach statistical significance ($r = .139, p = 0.107$).

Subjective Experience of Time Following Precuneus Lesions

In light of our lesion-symptom mapping findings in the precuneus, we performed a post-hoc review of medical records of 16 individuals following tumor removal that resulted in a focal lesion of the precuneus to evaluate if there were any observations of altered time perception. This cohort was described in detail previously.⁴² Time orientation was not systematically assessed in this retrospectively analyzed cohort, yet 2 individuals with left precuneus lesions that overlap with the lesion-symptom map findings spontaneously reported a notable change in their experience of time. One patient reported that “time did not run” and experienced subjective time dilation, experiencing minutes as hours. Days felt long to him and the time on his watch was systematically earlier than he expected. The second patient also spontaneously reported that “time did not run” and noted difficulties conceptualizing time, with his clinical notes also documenting trouble remembering the current date. While these 2 reports are anecdotal, they are aligned with the lesion-symptom map in supporting a role of the precuneus in influencing time perception and time orientation. The location of the tumor resection cavity for each patient is shown in Fig. 4C in relation to the lesion-symptom map results (in yellow). Verbal episodic memory was formally assessed in these 2 individuals using the Rappel libre/Rappel indicé à 16 items, (16-item Free and Cued Recall).

One of the 2 patients demonstrated no memory impairment (delayed free recall *z*-score of -0.71 ; >50 th percentile for total delayed recall after cueing). The other has a pronounced memory impairment with a delayed free recall *z*-score of -4.76 and was in the 1st percentile for total delayed recall after cueing.

Discussion

The main findings of our analysis are that damage to the MTL, precuneus, and regions of the ventromedial occipital lobe is associated with chronic time disorientation. The lesion network mapping results show that this pattern of results occur along a pathway connecting the MTL and precuneus. Our results also support prior work highlighting the role of the medial prefrontal cortex and mediodorsal nucleus of the thalamus in time orientation,^{14,15,17} but these findings were not represented in the lesion-symptom map. Other notable findings of interest include the observation of multiple risk factors for time disorientation, including: bilateral lesions, larger lesions (though we created a volume-matched comparison group), older age, and lesions from encephalitis, as has been reported previously.⁴³ Notably, time disoriented patients demonstrated overall higher levels of cognitive impairment relative to time oriented patients. This was especially true for co-occurring memory impairment, which was present in the majority of time disoriented patients (29 of 39 scored at least 2 standard deviations below average) and memory impairment had overlapping neuroanatomical correlates in the medial temporal lobes and ventral occipito-temporal pathway when mapped independently of time orientation.

The results in the precuneus are interesting in that they are present in smaller analyses limited to subjects without severe memory or cognitive impairment. Additional support for the possibility of precuneus involvement in time orientation came from a post-hoc analysis that identified 2 patients from an independent cohort with lesions involving this left precuneus region that spontaneously reported major distortions in their perception of time in the immediate days following the lesion onset, both reporting a subjective prolongation of their subjective experience relative to clock time. The functional connectivity network associated with this precuneus site partially overlaps with the default mode network, which includes medial temporal regions that were also implicated in time disorientation.

The precuneus has been implicated in time-related cognition from functional imaging studies,¹⁷ but this association with time disorientation has not been observed in lesions studies to our knowledge. The precuneus is a

highly connected region associated with complex information integration and has a high resting metabolic rate.⁴⁴ The functional role of the precuneus has been difficult to elucidate in part because focal lesions to the precuneus are extremely uncommon.⁴⁵ It is known to be involved in self-referential processes broadly,⁴⁴ including autobiographical memory.⁴⁶ In terms of time-related processing, an fMRI study showed activation in the precuneus in longer-scale temporal ordering tasks⁴⁷ and time orientation in healthy humans.¹⁷ Differences in precuneus activity were observed in relation to a time reproduction task in medicated and non-medicated patients with Parkinson's disease.⁴⁸

Regional findings in the parahippocampal gyrus and surrounding medial temporal cortex are in line with prior research suggesting that damage to and dysfunction of the MTL is associated with time disorientation across various etiologies.^{7,11,14} "Time cells" sensitive to duration have been identified in the MTL in rodents and humans,⁸⁻¹⁰ and degeneration of this system is associated with worsening time disorientation in patients with Alzheimer's disease.^{7,11}

We also observed regional findings in the ventromedial occipital lobe and extending anteriorly along the temporo-occipital junction, with the peak findings in the white matter. Our working interpretation of these findings is they result from lesions that disrupt communication between the other regional findings in the precuneus and MTL, yet we cannot rule out the possibility that this region is also important in time orientation independent of these other sites. There are proposals that vision and time-related processing may be interrelated, and our results are consistent with this possibility.^{7,44,49}

This study has limitations. First, while our overall sample size was large, there were only 39 individuals with time disorientation. This sample was even smaller in post-hoc analyses of individuals with relatively preserved cognition or without severe memory impairments, such that these analyses were underpowered. Second, we observed a strong relationship between time disorientation and memory impairment, such that we cannot confidently disentangle the neuroanatomical correlates of these 2 processes here. We had significant lesion-symptom maps of time disorientation and impaired memory that substantially overlapped. In contrast, a lesion-symptom map of time disorientation covarying for memory performance did not reach statistical significance. This could be consistent with time disorientation and memory sharing the same or partially overlapping neuroanatomical substrates, or this sample lacking the anatomical or behavioral resolution to disentangle these 2 constructs. A larger sample size with chronic time disorientation will be useful in further refining the underlying anatomy, ideally with additional

assessments of memory and attention. Related to sample size, we did not have sufficient lesion coverage of several brain regions that may support time orientation. Other studies have implicated the involvement of thalamic and cerebellar regions in time orientation; we lacked sufficient lesion coverage in these and potentially other regions to identify them in the lesion-symptom map. Third, chronic time disorientation can wax and wane over time. A patient may be more or less disoriented at the time of testing, and since test scores most contemporaneous with the scan date were utilized, scores could vary. But, orientation to time typically does not oscillate between disoriented and oriented, just in the degree of impairment.⁵⁰ Next, different timescales related to one's mental timeline may be represented differently in the brain. Long-term memory required for remembering the year may involve different brain regions compared to those important for shorter timescales like knowing the time on a clock. A future analysis of the neuroanatomical correlates of time disorientation at varying timescales would represent an improvement over the current binary categorization of an impaired and unimpaired group.

This study begins to formulate a neuroanatomical network important for time orientation. In doing so, it aligns with prior work implicating lesions of the medial temporal lobe, and we extend this work in also implicating the precuneus and medial occipito-temporal regions. With regard to how the human brain represents time, there are many outstanding questions that await future studies, including the neuroanatomy of other types of timing such as sub- and supra-second interval timing. We are optimistic a better understanding of these processes will continue to inform how the brain creates a temporal context for events and how these processes are utilized to support different domains of cognition.

Acknowledgments

This work was supported by the NIH NINDS division (R01NS114405), the Roy J. Carver Trust, and NIH Pre-doctoral Training Grant T32NS007421.

Author Contributions

J.S., J.B., D.T., and A.D.B. conceived of the project idea and designed the study. J.S., J.B., G.H., D.T., and A.D.B. acquired and analyzed the data. J.S. and A.D.B. drafted a significant portion of the manuscript and figures.

Potential Conflicts of Interest

No authors have any conflicts of interest to report.

References

- Benton AL, Van Allen MW, Fogel ML. Temporal orientation in cerebral disease. *J Nerv Ment Dis* 1964;139:110–119.
- Berrios GE. Orientation failures in medicine and psychiatry: discussion Paper1. *J R Soc Med* 1983;76:379–385.
- Guerrero-Berroa E, Luo X, Schmeidler J, et al. The MMSE orientation for time domain is a strong predictor of subsequent cognitive decline in the elderly. *Int J Geriatr Psychiatry* 2009;24:1429–1437.
- Liu P, Feng T. The effect of future time perspective on procrastination: the role of parahippocampal gyrus and ventromedial prefrontal cortex. *Brain Imaging Behav* 2019;13:615–622.
- Nan X, Qin Y. How thinking about the future affects our decisions in the present: effects of time orientation and episodic future thinking on responses to health warning messages. *Hum Commun Res* 2019;45:148–168.
- Eichenbaum H, Fortin N. Episodic memory and the hippocampus: It's about time. *Curr Dir Psychol Sci* 2003;12:53–57.
- El Haj M, Kapogiannis D. Time distortions in Alzheimer's disease: a systematic review and theoretical integration. *NPJ Aging Mech Dis* 2016;2:16016.
- Eichenbaum H. Time cells in the hippocampus: a new dimension for mapping memories. *Nat Rev Neurosci* 2014;15:732–744.
- Umbach G, Kantak P, Jacobs J, et al. Time cells in the human hippocampus and entorhinal cortex support episodic memory. *Proc Natl Acad Sci* 2020;117:28463–28474.
- Shimbo A, Izawa E-I, Fujisawa S. Scalable representation of time in the hippocampus. *Sci Adv* 2021;7:eabd7013.
- Daniel WF, Crovitz HF, Weiner RD. Neuropsychological aspects of disorientation. *Cortex* 1987;23:169–187.
- Dobbins IG, Rice HJ, Wagner AD, Schacter DL. Memory orientation and success: separable neurocognitive components underlying episodic recognition. *Neuropsychologia* 2003;41:318–333.
- Mahr JB, Greene JD, Schacter DL. A long time ago in a galaxy far, far away: how temporal are episodic contents? *Conscious Cogn* 2021;96:103224.
- Kumral E, Gulluoglu H, Dramali B. Thalamic chronotaxis: isolated time disorientation. *J Neurol Neurosurg Psychiatry* 2007;78:880–882.
- Parnaudeau S, Bolkan SS, Kellendonk C. The mediodorsal thalamus: an essential partner of the prefrontal cortex for cognition. *Biol Psychiatry* 2018;83:648–656.
- Hoffmann M. Chronotaxis: an underestimated right hemisphere syndrome (1364). *Neurology* 2020;94:1364.
- Peer M, Salomon R, Goldberg I, et al. Brain system for mental orientation in space, time, and person. *Proc Natl Acad Sci* 2015;112:11072–11077.
- High WM Jr, Levin HS, Gary HE Jr. Recovery of orientation following closed-head injury. *J Clin Exp Neuropsychol* 1990;12:703–714.
- Salisbury DB, Baños JH, Novack TA, Schneider JJ. Significance of decreased orientation performance during rehabilitation. *Rehabil Psychol* 2005;50:174–176.
- Pedersen PM, Jørgensen HS, Nakayama H, et al. Impaired orientation in acute stroke: frequency, determinants, and time-course of recovery. The copenhagen stroke study. *Cerebrovasc Dis* 1998;8:90–96.
- Boes AD, Prasad S, Liu H, et al. Network localization of neurological symptoms from focal brain lesions. *Brain* 2015;138:3061–3075.
- Bowren M Jr, Bruss J, Manzel K, et al. Post-stroke outcomes predicted from multivariate lesion-behaviour and lesion network mapping. *Brain* 2022;145:1338–1353.
- Tranel D. *Textbook of clinical neuropsychology*. New York, USA: Taylor & Francis, 2007.

24. Benton AL, Sivan AB, Hamsher KS, et al. *Contributions to neuropsychological assessment: a clinical manual*. New York, USA: Oxford University Press, 1994.
25. Staddon JE. Interval timing: memory, not a clock. *Trends Cogn Sci* 2005;9:312–314.
26. Frank RJ, Damasio H, Grabowski TJ. Brainvox: an interactive, multi-modal visualization and analysis system for neuroanatomical imaging. *Neuroimage* 1997;5:13–30.
27. Damasio H, Frank R. Three-dimensional in vivo mapping of brain lesions in humans. *Arch Neurol* 1992;49:137–143.
28. Smith SM, Jenkinson M, Woolrich MW, et al. Advances in functional and structural MR image analysis and implementation as FSL. *Neuroimage* 2004;23:S208–S219.
29. Pustina D, Avants B, Faseyitan OK, et al. Improved accuracy of lesion to symptom mapping with multivariate sparse canonical correlations. *Neuropsychologia* 2018;115:154–166.
30. Albazron FM, Bruss J, Jones RM, et al. Pediatric postoperative cerebellar cognitive affective syndrome follows outflow pathway lesions. *Neurology* 2019;93:e1561–e1571.
31. Cotovio G, Talmassov D, Barahona-Corrêa JB, et al. Mapping mania symptoms based on focal brain damage. *J Clin Invest* 2020;130:5209–5222.
32. Reich MM, Hsu J, Ferguson M, et al. A brain network for deep brain stimulation induced cognitive decline in Parkinson's disease. *Brain* 2022;145:1410–1421.
33. Boes AD, Fischer D, Geerling JC, et al. Connectivity of sleep- and wake-promoting regions of the human hypothalamus observed during resting wakefulness. *Sleep* 2018;41:41.
34. Fox MD, Snyder AZ, Vincent JL, et al. The human brain is intrinsically organized into dynamic, anticorrelated functional networks. *Proc Natl Acad Sci U S A* 2005;102:9673–9678.
35. Boes AD. Lesion network mapping: where do we go from here? *Brain* 2021;144:e5.
36. Winkler AM, Ridgway GR, Webster MA, et al. Permutation inference for the general linear model. *Neuroimage* 2014;92:381–397.
37. Horn A, Reich M, Vorwerk J, et al. Connectivity predicts deep brain stimulation outcome in Parkinson disease. *Ann Neurol* 2017;82:67–78.
38. Wechsler D. *Wechsler adult intelligence scale: WAIS-IV technical and interpretive manual*. London: Pearson, 2008.
39. Bowren M, Adolphs R, Bruss J, et al. Multivariate lesion-behavior mapping of general cognitive ability and its psychometric constituents. *J Neurosci* 2020;40:8924–8937.
40. Jenkinson M, Beckmann CF, Behrens TEJ, et al. FSL. *Neuroimage* 2012;62:782–790.
41. Tranel D, Vianna E, Manzel K, et al. Neuroanatomical correlates of the benton facial recognition test and judgment of line orientation test. *J Clin Exp Neuropsychol* 2009;31:219–233.
42. Herbet G, Lemaitre AL, Moritz-Gasser S, et al. The antero-dorsal precuneal cortex supports specific aspects of bodily awareness. *Brain* 2019;142:2207–2214.
43. Greenwood R, Bhalla A, Gordon A, Roberts J. Behaviour disturbances during recovery from herpes simplex encephalitis. *J Neurol Neurosurg Psychiatry Res* 1983;46:809.
44. Cavanna AE, Trimble MR. The precuneus: a review of its functional anatomy and behavioural correlates. *Brain* 2006;129:564–583.
45. Kumral E, Bayam FE, Özdemir HN. Cognitive and behavioral disorders in patients with precuneal infarcts. *Eur Neurol* 2021;84:157–167.
46. Hebscher M, Ibrahim C, Gilboa A. Precuneus stimulation alters the neural dynamics of autobiographical memory retrieval. *Neuroimage* 2020;210:116575.
47. Foudil S-A, Kwok SC, Macaluso E. Context-dependent coding of temporal distance between cinematic events in the human precuneus. *J Neurosci* 2020;40:2129–2138.
48. Dušek P, Jech R, Sieger T, et al. Abnormal activity in the precuneus during time perception in Parkinson's disease: an fMRI study. *PLoS One* 2012;7:e29635.
49. Kanai R, Paffen CL, Hogendoorn H, Verstraten FAJ. Time dilation in dynamic visual display. *J Vis* 2006;6:1421–1430.
50. Alverzo JP. A review of the literature on orientation as an indicator of level of consciousness. *J Nurs Scholarsh* 2006;38:159–164.